DMD #17533

BIOTRANSFORMATION OF LITHOCHOLIC ACID BY RAT HEPATIC MICROSOMES: METABOLITE ANALYSIS BY LC/MS

Anand K. Deo and Stelvio M. Bandiera

Faculty of Pharmaceutical Sciences, University of British Columbia, Vancouver, British

Columbia, Canada V6T 1Z3

1

Running Title:

Lithocholic acid biotransformation by hepatic P450 enzymes

Corresponding Author:

Stelvio M. Bandiera, Faculty of Pharmaceutical Sciences, University of British Columbia, 2146

East Mall, Vancouver, British Columbia, Canada V6T 1Z3. Telephone: 1-604-822-3815; Fax:

1-604-822-3035; Email: bandiera@interchange.ubc.ca

Number of text pages: 27 (not including tables, figure legends, or figures)

Number of tables: 2

Number of figures: 9

Number of references: 40 (max 40)

Number of words in the *Abstract*: 231 (max 250)

Number of words in the *Introduction*: 654 (max 750)

Number of words in the *Discussion*: 1498 (max 1500)

ABBREVIATIONS: CDCA, chenodeoxycholic acid; CYP, cytochrome P450; HDCA, hyodeoxycholic acid; MDCA, murideoxycholic acid; 3KCA, 3-keto-5β-cholanic acid; LC/MS, liquid chromatography/mass spectrometry; PB, phenobarbital; DEX, dexamethasone; MC, 3-methylcholanthrene; IgG, immunoglobulin G; α-MCA, α-muricholic acid; β-MCA, β-muricholic acid; γ-MCA, γ-muricholic acid; *m/z*, mass to charge ratio; UDCA, ursodeoxycholic acid; 6KLCA, 6-ketolithocholic acid; ILCA, isolithocholic acid; PXR, pregnane X receptor.

ABSTRACT:

Lithocholic acid is a lipid-soluble hepatotoxic bile acid that accumulates in the liver during cholestasis. A potential detoxification pathway for lithocholic acid involves hydroxylation by hepatic cytochrome P450 (CYP) enzymes. The purpose of the present study was to identify the hepatic microsomal metabolites of lithocholic acid by liquid chromatography-mass spectrometry and to determine the CYP enzymes involved. Incubation of lithocholic acid with rat hepatic microsomes and NADPH produced murideoxycholic acid (MDCA), isolithocholic acid (ILCA) and 3-keto-5β-cholanic acid (3KCA) as major metabolites, and 6-ketolithocholic acid (6KLCA) and ursodeoxycholic acid (UDCA) as minor metabolites. Experiments with hepatic microsomes prepared from rats pretreated with CYP inducers and with inhibitory antibodies indicated that CYP2C and CYP3A enzymes contribute to microsomal MDCA formation, while results obtained with a panel of recombinant CYP enzymes and CYP2D6 antiserum showed that CYP2D1 can also catalyze MDCA formation. Similar experimental evidence revealed that formation of 3KCA was mediated primarily by CYP3A enzymes. ILCA formation appeared to be catalyzed by a distinct pathway mediated largely by microsomal non-CYP enzymes. On the basis of the results obtained using lithocholic acid and 3KCA as substrates, a mechanism for the formation of ILCA involving a geminal diol intermediate is outlined. In conclusion, lithocholic acid was extensively metabolized by multiple CYP enzymes with the predominant biotransformation pathway being hydroxylation at the 6β-position. This study provides an insight into possible routes of detoxification of lithocholic acid.

Lithocholic acid (3α-hydroxy-5β-cholanic acid) is a hydrophobic bile acid that is formed by the dehydroxylation of chenodeoxycholic acid (3α,7α-dihydroxy-5β-cholanic acid, CDCA). Removal of the 7α-hydroxyl group of CDCA is catalyzed by hydratase enzymes associated with anaerobic bacteria that reside in the colon (Hofmann, 1999). Lithocholic acid is absorbed from the colon and transported to the liver, where the acidic moiety is conjugated with taurine or glycine before being excreted as a component of bile (Hofmann, 2002; Hofmann, 2004). Lithocholic acid, together with other biliary bile acids, facilitates the absorption, transport and distribution of lipid-soluble nutrients from the diet and aids in the elimination of cholesterol from the body (Hofmann, 1999). Figure 1 shows the chemical structures of lithocholic acid and other bile acids (Hofmann et al., 1992).

Lithocholic acid is present in human and rat liver at a concentration of approximately 1 to 5 nmol/g tissue, which represents approximately 4-5% of total bile acids in human and rat liver. In comparison, the major bile acids in human liver, which are cholic acid and CDCA, and the major bile acids in rat liver, which are cholic acid and muricholic acid, are present at concentrations that are 5 to 10 times greater (Setchell et al., 1997). Hepatic lithocholic acid concentrations are elevated in patients with cholestatic liver disease (Jezequel et al., 1994; Fischer et al., 1996; Erlinger, 1997; Hofmann, 2002; Berta et al., 2003; De Gottardi et al., 2004) and in rat models of biliary cholestasis (Setchell et al., 1997; Rost et al., 2003). The accumulation of lithocholic acid and other hydrophobic bile acids in liver has been implicated as a major factor contributing to liver injury in cholestasis because of the inherent cytotoxicity of this hydrophobic bile acid. Hepatic toxicity following chronic and acute administration of exogenous lithocholic acid or its conjugates is well documented in experimental animals (Javitt, 1966; Palmer and Ruban, 1966; Zaki et al., 1967; Miyai et al., 1971; Fischer et al., 1974).

The hepatotoxicity associated with lithocholic acid can be attenuated by hepatic biotransformation pathways including hydroxylation reactions catalyzed by the cytochrome P450 (CYP) enzymes and Phase II reactions involving conjugation of the 3α-hydroxyl group with sulfate (Kitada et al., 2003; Hofmann, 2004). The resulting metabolites are more water-soluble and more easily excreted. CYP-mediated hydroxylation has been proposed to be an effective detoxification mechanism in rodents and monkeys, whereas sulfate conjugation is considered to be a more important pathway in humans (Hofmann, 2004). There is evidence indicating that CYP-mediated hydroxylation of lithocholic acid is also prominent in humans. Lithocholic acid has been reported to be hydroxylated by human hepatic microsomes to hyodeoxycholic acid (HDCA), murideoxycholic acid (MDCA) and CDCA (Xie et al., 2001). Formation of HDCA was shown to be catalyzed primarily by human recombinant CYP3A4 (Araya and Wikvall, 1999; Xie et al., 2001). More recently, a different metabolite, 3-keto-5β-cholanic acid (3KCA), was identified as the major metabolite of lithocholic acid with human recombinant CYP3A4 (Bodin et al., 2005). In comparison, studies with rat liver microsomes demonstrated that 6β-hydroxylation of lithocholic acid leading to MDCA is the major pathway in the rat (Zimniak et al., 1989; Dionne et al., 1994). However, the CYP enzymes involved in the formation of MDCA in the rat were not identified.

In the present study, the hepatic metabolism of lithocholic acid was investigated in rat hepatic microsomes using a liquid chromatography/mass spectrometry (LC/MS)-based assay and the various CYP enzymes involved in metabolite formation were identified. Currently, mass spectrometry is one of the most sensitive and specific methods to quantify bile acids in tissue and subcellular fractions (Stedman et al., 2004). LC/MS was used to measure formation of the major and minor metabolites of lithocholic acid. Kinetic parameters associated with rates of metabolite formation in hepatic microsomes were also calculated. The hepatic CYP enzymes responsible

for metabolite formation were determined by a combination of approaches involving CYP inducer treatments, antibody inhibition experiments, and rat recombinant CYP enzymes.

Materials and Methods

Chemicals and reagents. Authentic bile acid standards were purchased from Steraloids Inc. (Newport, RI). Bile acid standards were dissolved in methanol as 1 mg/ml stock solutions. Additional dilutions were made in methanol for the biotransformation assay. Deuterated cholic-2,2,4,4-d_4 acid, which served as an internal standard, was a generous gift from Dr. Jan Palaty (Children's & Women's Health Center, Vancouver, BC, Canada). Sodium phenobarbital (PB) was obtained from BDH Chemicals (Toronto, Ontario, Canada). Dexamethasone (DEX) and 3-methylcholanthrene (MC) were purchased from Sigma-Aldrich Canada Ltd. (Oakville, Ontario, Canada). Baculovirus-insect cell control microsomes containing expressed rat CYP-oxidoreductase and baculovirus-insect cell microsomes containing expressed rat CYP enzymes, co-expressed with rat CYP-oxidoreductase or with rat CYP-oxidoreductase and rat cytochrome b_5 (BD SUPERSOMES™ Enzymes) were purchased from BD Biosciences (Oakville, Ontario, Canada). HPLC-grade chemicals and solvents were purchased from Fisher Scientific (Ottawa, Ontario, Canada).

Rabbit CYP2D6 polyclonal antiserum (Daiichi Pure Chemicals Co. Ltd., Tokyo) was purchased from BD Biosciences. The reaction of CYP2D6 antiserum with rat CYP2D1 was assessed in our laboratory by immunoblot analysis using recombinant rat CYP enzymes. Rabbit anti-rat CYP2C polyspecific immunoglobulin G (IgG) and rabbit anti-rat CYP3A polyspecific IgG were prepared as described previously (Panesar et al., 1996; Wong and Bandiera, 1996). The inhibitory activities of the anti-CYP2C and anti-CYP3A IgG preparations toward rat hepatic microsomal testosterone 2α- and 16α-hydroxylation and testosterone 6β-hydroxylation,

6

respectively, had been determined previously (Law, 1995; Wong and Bandiera, unpublished results).

Animal treatment and preparation of hepatic microsomes. Male and female Long-Evans, male Wistar and male Sprague Dawley rats (7-8 weeks of age) were purchased from Charles River Canada Inc. (Saint-Constant, Quebec, Canada). Upon arrival, rats were housed in pairs in polycarbonate cages on corncob bedding (Anderson's Maumee, OH) with free access to water and food (Laboratory Rodent Diet, PMI Feeds Inc., Richmond, IN). Animal quarters were maintained at a constant temperature (23°C) with controlled light (14 h) and dark (10 h) cycles. Rats were cared for in accordance with the principles and guidelines of the Canadian Council on Animal Care.

Male or female Long-Evans rats (n ≥ 5) were treated with xenobiotics as follows: PB (dissolved in water, 75 mg/kg/day), MC (dissolved in corn oil, 25 mg/kg/day), DEX (dissolved in corn oil, 100 mg/kg/day) or vehicle (0.8 ml/kg/day). Compounds were administered by intraperitoneal injection for 4 days and rats were killed by decapitation 24 h after the last treatment. Microsomes were prepared from pooled livers as described previously (Thomas et al., 1983). Microsomes were also prepared from pooled livers from untreated Wistar rats (n=16) or Sprague Dawley rats (n=4). Microsomal pellets were suspended in 0.25 M sucrose and aliquots were stored at –75°C, until needed. Protein concentration was measured by the method of Lowry et al. (1951) using bovine serum albumin as a standard.

Lithocholic acid biotransformation assay. Reaction mixtures contained lithocholic acid (0.5–300 μM), 0.5 mg of hepatic microsomal protein, 50 mM potassium phosphate buffer, pH 7.4, 3 mM magnesium chloride, and 1 mM NADPH in a final volume of 1 ml. After preincubation for

10 min at room temperature, reactions were initiated with NADPH and allowed to proceed for 30 min at 37°C. Reactions were terminated with 4 ml of dichloromethane:isopropanol (80:20). A fixed amount (0.4 μg) of internal standard (cholic-2,2,4,4-d$_4$ acid) was then added to each sample. Tubes were vortex-mixed for 1 min, shaken manually for 1 min and spun at 2000 *g* for 5 min. The top aqueous layer was carefully removed, placed into a clean tube and re-extracted with a second 4 ml aliquot of dichloromethane:isopropanol (80:20). The final aqueous phase was discarded and the organic phase from the second and first extraction were combined and evaporated to dryness with nitrogen. The residue was reconstituted in 0.2 ml of mobile phase (methanol:water:10 mM ammonium acetate, pH 4.6 (67:23:10)) and filtered through a 3 mm, 0.45 μm syringe polytetrafluoroethylene filter. A 10 μl aliquot of each sample was analyzed by LC/MS as described by Stedman et al. (2004) with modifications as outlined below.

Control samples devoid of substrate, NADPH or microsomes, and defined mixtures of authentic bile acid standards, were routinely included in each assay. Incubations with rat recombinant CYP enzymes, instead of rat hepatic microsomes, were also carried out. Reaction mixtures contained 30 pmoles of each recombinant CYP enzyme (CYP1A2, CYP2A2, CYP2B1, CYP2C6, CYP2C11, CYP2C13, CYP2D1, CYP3A1 or CYP3A2) or, in the case of insect cell control microsomes, an equivalent amount of protein (0.15 mg). To determine if metabolite formation was CYP-mediated, preliminary experiments were conducted with carbon monoxide-treated hepatic microsomes or heat-denatured microsomes. Microsome samples were boiled for 5 min in assay buffer. Carbon monoxide was bubbled into an incubation mixture containing assay buffer and microsomes for 2 min.

Assay conditions were tested using microsomes from untreated male Wistar rats to ensure that substrate and cofactor concentrations were saturating and that product formation was linear

with respect to incubation time (1 to 60 min) and protein concentration (0.25 to 2 mg/ml of reaction mixture).

Antibody inhibition. The lithocholic acid biotransformation assay was performed as described above except that microsomes were preincubated with rabbit anti-rat CYP2C IgG, anti-rat CYP3A IgG or control IgG for 15 min at room temperature prior to addition of substrate. NADPH was added to initiate the reaction. Four concentrations of each IgG (0, 1, 2.5 and 5.0 mg IgG/mg of microsomal protein) were tested. Formation of MDCA by rat hepatic microsomes or recombinant CYP2D1 was measured in the presence of rabbit CYP2D6 antiserum or control serum. Hepatic microsomes or recombinant CYP2D1 were preincubated with various amounts of either rabbit CYP2D6 antiserum or control serum (0, 10, 25, 50 and 100 µl/ml reaction mixture) for 15 min at room temperature prior to addition of lithocholic acid. Reactions were initiated with NADPH.

Analytical methods. Formation of lithocholic acid metabolites was analyzed by LC/MS. Lithocholic acid and its metabolites were resolved on a XTerra™ MS C18 (2.1 mm × 150 mm, 3.5 µm) column (Waters, Milford, MA) at 40°C using a Hewlett-Packard model 1090 II liquid chromatograph (Avondale, PA). The mobile phase consisted of solvent A (methanol:water:10 mM ammonium acetate, pH 4.6 (50:40:10)) and solvent B (methanol:water:10 mM ammonium acetate, pH 4.6 (85:5:10)). A linear gradient was used starting from 100% solvent A to 100% solvent B from 0 to 20 min, 100% solvent B from 20 to 25 min, followed by an abrupt return to 100% solvent A at 25 min, and re-equilibration with 100% solvent A for 10 min. The flow rate was maintained at 0.15 ml/min and total run time was 35 min/sample. The LC was interfaced to a Fisons VG Quattro mass detector (Fisons Instruments, VG-Analytical, Manchester, United

Kingdom). The MS was operated in atmospheric pressure electrospray negative ionization mode, with bath gas flow and nebulizer gas flow rates of 250 l/hr and 20 l/hr, respectively, a source temperature of 160°C, and capillary and cone voltages of 3 kV and 40 V, respectively. MASSLYNX® v3.1 software (Micromass, Altrincham, United Kingdom) was used for data acquisition.

Metabolites were identified by comparison of their retention times and mass to charge ratios (*m/z*) with those of authentic standards. Quantitative determination of bile acids was performed by selected negative ion monitoring at *m/z* of 411, 407, 391, 389, 375 and 373. Under these conditions, the internal standard, cholic-2,2,4,4-d$_4$ acid (MW 412.57), typically eluted at 17 min and was monitored at *m/z* 411. α-Muricholic acid (α-MCA, MW 408.57), β-muricholic acid (β-MCA, MW 408.57), γ-muricholic acid (γ-MCA, MW 408.57) and cholic acid (MW 408.57) eluted at 12, 13, 15 and 17 min, respectively, and were monitored at *m/z* 407. MDCA (MW 392.57), ursodeoxycholic acid (UDCA, MW 392.57), HDCA (MW 392.57), CDCA (MW 392.57) and deoxycholic acid (MW 392.57) eluted at 11, 15, 17, 20 and 20.5 min, respectively, and were monitored at *m/z* 391. 6-Ketolithocholic acid (6KLCA, MW 390.56) eluted at 15 min and was monitored at *m/z* 389. Isolithocholic acid (ILCA, MW 376.57) and lithocholic acid (MW 376.57) eluted at 23 and 26 min, respectively, and were monitored at *m/z* 375. 3KCA (MW 374.56) eluted at 25 min and was monitored at *m/z* 373. Metabolites were quantified from calibration plots of the peak area ratio of the authentic standard and internal standard plotted against the concentration of the authentic standard.

Data analysis and calculation of enzyme kinetic parameters. Data were analyzed using the SigmaPlot® Enzyme Kinetics Module (v.1.1, Systat Software Inc., Richmond, CA). Metabolite formation as a function of substrate concentration was analyzed by nonlinear regression analysis

10

and apparent K_m, K' and V_{max} values were generated using the Hill equation (Equation 1) or the substrate inhibition kinetic equation (Equation 2) for the major metabolites, or the Michaelis-Menten equation (Equation 3) for the minor metabolites of lithocholic acid.

$$v = \frac{V_{max} \times [S]^n}{K' + [S]^n} \qquad \text{(Equation 1)}$$

$$v = \frac{V_{max}}{1 + K_m/[S] + [S]/K_i} \qquad \text{(Equation 2)}$$

$$v = \frac{V_{max} \times [S]}{K_m + [S]} \qquad \text{(Equation 3)}$$

where v is initial velocity of the reaction, V_{max} is the maximal velocity, $[S]$ is the substrate concentration, K' is the Hill dissociation constant, n is the Hill coefficient representing cooperativity of the reaction, K_m is the Michaelis-Menten constant, and K_i is the dissociation constant of substrate binding to the inhibitory site.

Statistical analysis. Comparisons of rates of metabolite formation were made using the unpaired t test with Welch's correction. A p value of < 0.05 was considered statistically significant.

Results

Biotransformation of lithocholic acid and metabolite identification. A mixture of thirteen bile acid standards (α-MCA, β-MCA, γ-MCA, cholic acid, MDCA, UDCA, HDCA, CDCA, deoxycholic acid, 6KLCA, ILCA, 3KCA and lithocholic acid) was initially analyzed to ensure that potential metabolites were resolved with the LC conditions selected. Baseline separation of

the bile acid standards was achieved, with the exception of α-MCA and β-MCA, which were distinguished by spiking with authentic standards.

Incubation of lithocholic acid with liver microsomes from male Wistar rats yielded seven metabolites that were identified as β-MCA, MDCA, ILCA, UDCA, HDCA, 6KLCA and 3KCA (Fig. 2) by comparison with authentic standards. The major metabolites were MDCA, ILCA and 3KCA. 6KLCA and UDCA were minor metabolites, while β-MCA and HDCA were produced at levels close to or below the limit of quantification. Four other peaks (M-1, m/z 407; M-2, m/z 407; M-3, m/z 391 and M-4, m/z 389) corresponding to trace metabolites were detected but were not identified because the retention times of these metabolites did not match those of the authentic standards. To determine if lithocholic acid biotransformation differed among rat strains, incubations were performed with hepatic microsomes from male Wistar, Long-Evans and Sprague Dawley rats. The same metabolite profile was obtained for all three rat strains (results not shown). Metabolite formation was not observed when lithocholic acid was incubated with carbon monoxide-treated or boiled microsomal preparations, or when NADPH was omitted from the reaction mixture.

Although CDCA was previously reported to be a metabolite of lithocholic acid in the rat (Zimniak., 1989), our results indicate that CDCA is not a metabolite. A peak at m/z 391 with the same retention time as CDCA was observed but was determined to be a contaminant of lithocholic acid as it was detected with reaction mixtures that contained substrate and NADPH but not hepatic microsomes and the area of the CDCA peak did not change following incubation with increasing concentrations of hepatic microsomes.

Kinetic analysis of hepatic microsomal metabolite formation. Formation of the major and minor metabolites of lithocholic acid was evaluated over a range of substrate concentrations (0.5

to 300 μM). An incubation time of 30 min and a microsomal protein concentration of 0.5 mg/ml were found to be optimal and were used in subsequent experiments. A lithocholic acid concentration of 100 or 250 μM, depending on the metabolite, was found to be saturating. Hepatic microsomal MDCA formation exhibited typical Michaelis-Menten kinetics up to a substrate concentration of 100 μM. At higher concentrations of lithocholic acid, the rate of MDCA formation decreased, possibly as a result of substrate inhibition (Fig. 3A). Formation of ILCA and 3KCA exhibited sigmoidal kinetic profiles. Decreased ILCA and 3KCA formation was observed at substrate concentrations greater than 100 μM for ILCA and 250 μM for 3KCA (Fig. 3B and 3C). Hence, saturating substrate concentrations of 100 μM for MDCA and ILCA formation and 250 μM for 3KCA formation were selected for further experiments. Nonlinear Eadie-Hofstee plots of MDCA, ILCA and 3KCA formation, signifying atypical enzyme kinetics, were obtained (Fig. 3A, 3B and 3C). Of the minor metabolites that could be quantified, formation of 6KLCA and UDCA followed typical Michaelis-Menten kinetics up to a substrate concentration of 100 μM (results not shown).

Apparent K_m and V_{max} values for hepatic microsomal MDCA formation were calculated using equation 2. Apparent K' and V_{max} values for hepatic microsomal ILCA and 3KCA formation were calculated using equation 1 (Table 1). Positive cooperativity ($n > 2$) was indicated for ILCA and 3KCA formation. The apparent V_{max} value for MDCA formation was approximately 7 and 14 times higher than the values for ILCA and 3KCA formation, respectively, demonstrating that MDCA was the predominant microsomal metabolite of lithocholic acid in rats. On the other hand, the lower apparent K' value associated with ILCA formation (29.3 ± 5.9 μM) suggests that this metabolite would be preferentially formed at low lithocholic acid concentrations. The apparent V_{max} values calculated for UDCA and 6KLCA

13

formation (Table 1) confirm that formation of these metabolites was quantitatively less important than formation of MDCA, ILCA or 3KCA.

Effect of CYP inducers on lithocholic acid biotransformation. To identify the CYP enzymes involved in lithocholic acid biotransformation, experiments were performed with hepatic microsomes prepared from male and female Long-Evans rats that had been pretreated with MC, PB or DEX. Comparison of rates of formation of the metabolites revealed a distinct sex difference for some of the metabolites (Table 2). Rates of MDCA and ILCA formation for control male rats were approximately 2 and 30 times greater, respectively, than for control female rats, whereas the rate of formation of 3KCA was similar for control male and female rats. Treatment with PB or MC decreased formation rates of MDCA and ILCA for male rats. The rate of formation of 3KCA was slightly, but not significantly, greater for both sexes following DEX treatment, while formation of MDCA and ILCA was not affected. With respect to the minor metabolites, rates of formation of 6KLCA and UDCA were greater for male than female rats and formation of both metabolites was increased following treatment with DEX, but not PB or MC (data not shown).

Antibody inhibition studies. The role of CYP2C and CYP3A enzymes in lithocholic acid biotransformation was investigated using antibodies against CYP2C and CYP3A enzymes. Rates of formation of MDCA and 3KCA were each inhibited by approximately 50% by anti-CYP2C IgG (at 5 mg IgG/mg protein), whereas ILCA formation was not affected (Fig. 4). Anti-CYP3A IgG (at 5 mg IgG/mg protein) inhibited the rates of formation of MDCA, ILCA and 3KCA by 40 to 60% (Fig. 4). Formation of 6KLCA and UDCA were not affected by anti-

14

CYP2C IgG but were inhibited by approximately 20% and 30%, respectively, following

incubation of microsomes with anti-CYP3A IgG (at 5 mg IgG/mg protein, data not shown).

Biotransformation studies with recombinant CYP enzymes. The contribution of individual

CYP enzymes in lithocholic acid biotransformation was evaluated using a panel of nine rat

recombinant CYP enzymes (Fig. 5). Initial experiments were conducted to determine CYP

concentrations that would ensure linearity of product formation with incubation time. An

incubation time of 30 min and rat recombinant CYP enzyme concentration of 30 pmol CYP/ml

were found to be optimal. Under the experimental conditions employed, CYP2D1 was the most

active CYP enzyme catalyzing MDCA formation. In comparison, formation of ILCA was

catalyzed at a relatively low rate by several recombinant CYP enzymes including CYP1A2,

CYP2C6, CYP2D1, CYP3A1 and CYP3A2, but not by CYP2A2 or CYP2C13. The rate of

formation of ILCA by the recombinant CYP enzymes was approximately 4 to 16 times less than

the rate obtained with hepatic microsomes, when activity values were expressed per nmol total

CYP. CYP3A2, followed by CYP3A1 and CYP2C11, were the most active CYP enzymes

catalyzing 3KCA formation. The rate of 3KCA formation by recombinant CYP3A2 was found

to be greater, when expressed per nmol total CYP, than that obtained with hepatic microsomes

(approximately 31 vs 0.6 pmol/min/pmol CYP, respectively). Formation of 6KLCA and UDCA

by rat recombinant CYP enzymes was also assessed. 6KLCA formation was catalyzed mainly

by CYP3A1 and CYP3A2, while UDCA formation was catalyzed solely by CYP2A2 (results not

shown). There was no evidence of β-MCA or CDCA formation by the rat recombinant CYP

enzymes.

To verify the involvement of CYP2D1 in MDCA formation, antibody inhibition

experiments were conducted using CYP2D6 antiserum, which has been reported to cross-react

with CYP2D1 (Umehara et al., 1997). MDCA formation by recombinant CYP2D1 was inhibited

by 90% at the highest concentration of CYP2D6 antiserum tested (Fig. 7). In contrast, CYP2D6

antiserum had no effect on MDCA formation by hepatic microsomes.

Conversion of lithocholic acid to ILCA involves epimerization of the hydroxyl group at

the 3-position. To determine if ILCA formation could occur by a stepwise process, 3KCA was

incubated with hepatic microsomes prepared from control male rats and with a panel of rat

recombinant CYP enzymes. Hepatic microsomes catalyzed ILCA formation from both

lithocholic acid and 3KCA. Formation of ILCA from 3KCA was not catalyzed by any of the

recombinant CYP enzymes. Formation of 3KCA by recombinant CYP3A2 was further

evaluated at substrate concentrations of 0.5 to 100 μM (Fig. 6). Formation of 3KCA by

recombinant CYP3A2 followed typical Michaelis-Menten kinetics, which is in contrast to the

atypical sigmoidal kinetic pattern observed with hepatic microsomes. These data suggest that

formation of 3KCA in hepatic microsomes involved more than a single CYP enzyme. A V_{max}

value of 31.5 pmol/min/pmol CYP and a K_m value of 18.9 μM were obtained for 3KCA

formation by recombinant CYP3A2.

DISCUSSION

Lithocholic acid was extensively metabolized by rat hepatic microsomes to three major (MDCA,

ILCA and 3KCA) and two minor (6KLCA and UDCA) products, as determined by LC/MS. The

predominant biotransformation pathway involved hydroxylation of lithocholic acid at the 6β-

position and led to formation of MDCA. This result is consistent with previous in vivo and in

vitro studies, which described hepatic 6β-hydroxylation of bile acids as a major pathway in rat

(Voigt et al., 1968; Gustafsson, 1978) and identified MDCA as a major metabolite of lithocholic

acid (Zimniak et al., 1989; Dionne et al., 1994). However, the CYP enzymes catalyzing MDCA

formation were not identified in previous studies. Our experiments with hepatic microsomes prepared from rats pretreated with CYP inducers and with inhibitory CYP antibodies indicated that CYP2C and CYP3A enzymes contribute to microsomal MDCA formation, while results obtained with a panel of rat recombinant CYP enzymes showed that CYP2D1 also catalyzes MDCA formation. The lack of effect by CYP2D6 antiserum on hepatic microsomal MDCA formation suggests that there is little or no contribution by CYP2D1 to the activity of hepatic microsomes. This may be explained by the relatively low level of expression of CYP2D1. Determination of CYP2D1 levels in hepatic microsomes by immunoblot analysis indicated that CYP2D1 accounted for approximately 2-4% of total CYP in hepatic microsomes prepared from untreated Wistar and Long-Evans rats (results not shown). Collectively, the results imply that several CYP enzymes, which are expressed at higher levels than CYP2D1, are involved in MDCA formation as shown in Fig. 5A.

Lithocholic acid concentrations of 5 to 10 µM have been reported in the liver of cholestatic patients and in rat models of biliary cholestasis (Jezequel et al., 1994; Fischer et al., 1996; Erlinger, 1997; Setchell et al., 1997; Hofmann, 2002; Berta et al., 2003; Rost et al., 2003; De Gottardi et al., 2004). A lithocholic acid concentration of 100 µM was found to be saturating for hepatic microsomal MDCA formation in the present study. Nevertheless, MDCA was the major metabolite obtained in the in vitro biotransformation assay, with a rate of formation of 250-500 pmol/min/mg at a lithocholic acid concentration of 5 µM, which approximates the physiological hepatic concentration. Thus, our study demonstrates that 6β-hydroxylation is the major CYP-mediated hepatic pathway of lithocholic acid biotransformation in the rat. In comparison, hydroxylation of lithocholic acid at the 6α-position has been proposed to be the

predominant CYP-mediated pathway in humans (Araya and Wikvall, 1999; Xie et al., 2001). Only a trace amount of HDCA was produced by rat liver microsomes in the present study.

ILCA, the 3β-isomer of lithocholic acid, was the second most abundant microsomal metabolite detected in our study. ILCA was reported to be a major metabolite in human feces (Norman and Palmer, 1964; Palmer, 1971) and was identified as an in vivo metabolite of rats fed sulfated lithocholic acid (Palmer, 1971; Zimniak et al., 1989; Dionne et al., 1994) but was not found to be a metabolite of lithocholic acid produced by rat liver microsomes (Palmer, 1971; Zimniak et al., 1989; Dionne et al., 1994). In our study, conversion of lithocholic acid to ILCA was observed with some rat recombinant CYP enzyme preparations but at a relatively low rate. Hepatic microsomal ILCA formation was not induced by pretreatment with MC, PB or DEX, was not inhibited by anti-CYP2C IgG and was slightly inhibited by anti-CYP3A IgG. The results suggest that microsomal enzymes other than CYP enzymes were involved in ILCA formation. Epimerization of the hydroxyl group on steroid molecules is most often catalyzed by hepatic hydroxysteroid dehydrogenase and steroid oxidoreductase enzymes and is not a common CYP-mediated reaction (Penning et al., 1986). A possible mechanism for the formation of ILCA is shown in Fig. 8. We speculate that microsomal ILCA formation can proceed by two pathways. One pathway involves conversion of lithocholic acid to ILCA, possibly through a geminal diol intermediate with subsequent loss of a hydroxyl group. The geminal diol is formed by β–hydroxylation at an existing α–hydroxy position (as suggested by Bodin et al., 2005). The geminal diol intermediate can spontaneously rearrange to form either ILCA or 3KCA. A second pathway involves 3β-oxidation of lithocholic acid followed by dehydration to form 3KCA, with subsequent reduction of 3KCA to ILCA. Our experiments conducted using 3KCA as substrate showed that although ILCA is a major hepatic microsomal metabolite of 3KCA, none of the recombinant CYP enzymes contributed significantly to that conversion. Accordingly, we believe

that both pathways are mediated largely by non-CYP enzymes. An example of a microsomal enzyme that can catalyze this reaction is 3β-hydroxy-Δ^5-C_{27}-steroid oxidoreductase enzyme, which was purified from rabbit liver microsomes and was shown to catalyze the reversible oxidation of the 3β-hydroxyl group of C_{27}-steroids (Wikvall, 1981).

3KCA was the third most abundant hepatic microsomal metabolite of lithocholic acid in our study. A recent report identified 3KCA as the major lithocholic acid metabolite (74% of total) formed by human recombinant CYP3A4 (Bodin et al., 2005), and two earlier studies found 3KCA as a major in vivo product of rats fed a lithocholic acid-enriched diet (Thomas et al., 1964; Sakai et al., 1980). Formation of 3KCA from lithocholic acid entails oxidation of a hydroxyl group and can be catalyzed by CYP enzymes by the mechanism described above. In the present study, treatment of male and female rats with DEX led to increased 3KCA formation suggesting that CYP3A enzymes contribute to formation of this metabolite. Results of the antibody inhibition experiments substantiate the involvement of CYP3A and CYP2C in 3KCA formation. Of the recombinant enzymes examined, the highest catalytic activity was obtained with CYP3A2. Taken together, the data provide convincing evidence that 3KCA formation in rat hepatic microsomes was catalyzed primarily by CYP3A. A proposed mechanism for 3KCA formation was outlined above (see Fig. 8).

Minor metabolites, namely 6KLCA and UDCA, as well as metabolites that were detected but could not be quantified, namely HDCA and β-MCA, were also reported by Zimniak et al. (1989). Our results suggest that 6KLCA formation was catalyzed mainly by CYP3A enzymes, while UDCA formation was catalyzed by CYP2A enzymes. Appreciable formation of β-MCA was apparent only at low substrate concentrations suggesting that β-MCA was converted to other metabolites. CDCA, which was reported to be a metabolite in previous studies (Thomas et al.,

1964; Zimniak et al., 1989), was identified herein as a contaminant of lithocholic acid. We found no evidence of CDCA formation by either rat hepatic microsomes or rat recombinant CYP enzymes.

Our study focused primarily on the contribution of CYP enzymes to the biotransformation of lithocholic acid in hepatic microsomes. We are aware that Phase II enzymes such as sulfotransferases and glucuronosyl transferases also play an important role in lithocholic acid biotransformation. Glucuronosyl transferases are microsomal enzymes that may facilitate conversion of lithocholic acid and its metabolites, such as MDCA, to their ester glucuronide conjugates, thereby affecting MDCA formation. Moreover, nuclear hormone receptors, such as the pregnane X receptor (PXR), constitutive androstane receptor, liver X receptor, and farnesoid X receptor can be activated by bile acids and help regulate bile acid homeostasis (Staudinger et al., 2001; Makishima, 2005). Some of these receptors, such as PXR, are involved in the inducible expression of CYP enzymes and Phase II enzymes, such as sulfotransferases and glucuronosyl transferases (Tien and Negishi, 2006). Thus, treatment with DEX and other inducers used in the present study could alter formation of metabolites such as MDCA through an effect on Phase II enzymes, apart from the effect on CYP enzymes. This may partly explain the decreased MDCA formation observed after pretreatment with DEX. The concentration of DEX used in our study (100 mg/kg) is sufficient enough to activate PXR in rodents (Hartley et al., 2004).

In summary, LC/MS proved to be an effective method for resolving and identifying the biotransformation products of lithocholic acid. Lithocholic acid, like many CYP substrates, is metabolized by multiple CYP enzymes, which catalyze overlapping pathways. Our study suggests a major role for hepatic CYP2C and CYP3A enzymes in lithocholic acid biotransformation. In rats and humans, the contribution of individual CYP enzymes to the

various metabolic pathways is determined by their level of expression and the tissue concentration of lithocholic acid. CYP2C enzymes are the predominant CYP enzyme subfamily expressed in untreated rat liver and together with CYP3A enzymes, which predominate in human liver, are expected to be the main catalysts of lithocholic acid biotransformation in rats and possibly in humans. Because CYP3A is involved in the formation of most of the major metabolites of lithocholic acid, induction of CYP3A enzymes offers a potential mechanism to lessen the hepatotoxicity associated with high tissue levels of lithocholic acid. On the basis of results obtained, a scheme for CYP-mediated formation of major lithocholic acid metabolites in rat hepatic microsomes is proposed in Fig. 9.

The LC/MS analytical method employed herein provides a sound foundation for future bile acid biotransformation studies using human hepatic microsomes and purified or recombinant CYP enzymes, studies that are currently underway in our laboratory.

ACKNOWLEDGMENTS

The authors thank Dr. Frank S. Abbott and Mr. Roland Burton, UBC, Faculty of Pharmaceutical Sciences, for guidance and technical help with the LC/MS analysis. We thank Dr. Jan Palaty, Children's & Women's Health Centre of British Columbia, for supplying us with the cholic-2,2,4,4-d_4 acid internal standard. We are also indebted to Dr. Eugene Hrycay and Patrick R. Edwards for their helpful comments during the preparation of the manuscript.

REFERENCES

Araya Z and Wikvall K (1999) 6alpha-hydroxylation of taurochenodeoxycholic acid and lithocholic acid by CYP3A4 in human liver microsomes. *Biochim Biophys Acta* **1438:**47-54.

Berta L, Fronticelli Baldelli C, Fazzari A, Radice E, Bargoni A, Frairia R and Gaetini A (2003) Sex steroid receptors, secondary bile acids and colorectal cancer. A possible mechanism of interaction. *Panminerva Med* **45:**261-266.

Bodin K, Lindbom U and Diczfalusy U (2005) Novel pathways of bile acid metabolism involving CYP3A4. *Biochim Biophys Acta* **1687:**84-93.

De Gottardi A, Touri F, Maurer CA, Perez A, Maurhofer O, Ventre G, Bentzen CL, Niesor EJ and Dufour JF (2004) The bile acid nuclear receptor FXR and the bile acid binding protein IBABP are differently expressed in colon cancer. *Dig Dis Sci* **49:**982-989.

Dionne S, Tuchweber B, Plaa GL and Yousef IM (1994) Phase I and phase II metabolism of lithocholic acid in hepatic acinar zone 3 necrosis. Evaluation in rats by combined radiochromatography and gas-liquid chromatography-mass spectrometry. *Biochem Pharmacol* **48:**1187-1197.

Erlinger S (1997) Drug-induced cholestasis. *J Hepatol* **26 Suppl 1:**1-4.

Fischer CD, Cooper NS, Rothschild MA and Mosbach EH (1974) Effect of dietary chenodeoxycholic acid and lithocholic acid in the rabbit. *Am J Dig Dis* **19:**877-886.

Fischer S, Beuers U, Spengler U, Zwiebel FM and Koebe HG (1996) Hepatic levels of bile acids in end-stage chronic cholestatic liver disease. *Clin Chim Acta* **251:**173-186.

Gustafsson J (1978) Effect of biliary obstruction on 26-hydroxylation of C27-steroids in bile acid synthesis. *J Lipid Res* **19:**237-243.

Hartley DP, Dai X, He YD, Carlini EJ, Wang B, Huskey SE, Ulrich RG, Rushmore TH, Evers R

and Evans DC (2004) Activators of the rat pregnane X receptor differentially modulate

hepatic and intestinal gene expression. *Mol Pharmacol* **65:**1159-1171.

Hofmann AF (1999) The continuing importance of bile acids in liver and intestinal disease. *Arch

Intern Med* **159:**2647-2658.

Hofmann AF (2002) Cholestatic liver disease: pathophysiology and therapeutic options. *Liver* **22

Suppl 2:**14-19.

Hofmann AF (2004) Detoxification of lithocholic acid, a toxic bile acid: relevance to drug

hepatotoxicity. *Drug Metab Rev* **36:**703-722.

Hofmann AF, Sjovall J, Kurz G, Radominska A, Schteingart CD, Tint GS, Vlahcevic ZR and

Setchell KD (1992) A proposed nomenclature for bile acids. *J Lipid Res* **33:**599-604.

Javitt NB (1966) Cholestasis in rats induced by taurolithocholate. *Nature* **210:**1262-1263.

Jezequel AM, Benedetti A, Bassotti C and Orlandi F (1994) *Drug induced cholestasis*. Elsevier

Science BV, Netherlands.

Kitada H, Miyata M, Nakamura T, Tozawa A, Honma W, Shimada M, Nagata K, Sinal CJ, Guo

GL, Gonzalez FJ and Yamazoe Y (2003) Protective role of hydroxysteroid

sulfotransferase in lithocholic acid-induced liver toxicity. *J Biol Chem* **278:**17838-17844.

Law E (1995) Effect of Cimetidine On Hepatic Cytochrome P450 1A and P450 2C in Male

Rats., in *M.Sc. Thesis*, Faculty of Pharmaceutical Sciences, University of British

Columbia, Vancouver, BC, Canada.

Lowry OH, Rosebrough NJ, Farr AL, Randall RJ (1951) Protein measurement with the folin

phenol reagent. *J Biol Chem* **193:**265-275.

24

Makishima M (2005) Nuclear receptors as targets for drug development: regulation of cholesterol and bile acid metabolism by nuclear receptors. *J Pharmacol Sci* **97:**177-183.

Miyai K, Price VM and Fisher MM (1971) Bile acid metabolism in mammals. Ultrastructural studies on the intrahepatic cholestasis induced by lithocholic and chenodeoxycholic acids in the rat. *Lab Invest* **24:**292-302.

Norman A and Palmer RH (1964) Metabolites of Lithocholic Acid-24-C-14 in Human Bile and Feces. *J Lab Clin Med* **63:**986-1001.

Palmer RH (1971) Bile acid sulfates. II. Formation, metabolism, and excretion of lithocholic acid sulfates in the rat. *J Lipid Res* **12:**680-687.

Palmer RH and Ruban Z (1966) Production of bile duct hyperplasia and gallstones by lithocholic acid. *J Clin Invest* **45:**1255-1267.

Panesar SK, Bandiera SM and Abbott FS (1996) Comparative effects of carbamazepine and carbamazepine-10,11-epoxide on hepatic cytochromes P450 in the rat. *Drug Metab Dispos* **24:**619-627.

Penning TM, Smithgall TE, Askonas LJ and Sharp RB (1986) Rat liver 3 alpha-hydroxysteroid dehydrogenase. *Steroids* **47:**221-247.

Rost D, Herrmann T, Sauer P, Schmidts HL, Stieger B, Meier PJ, Stremmel W and Stiehl A (2003) Regulation of rat organic anion transporters in bile salt-induced cholestatic hepatitis: effect of ursodeoxycholate. *Hepatology* **38:**187-195.

Sakai K, Makino T, Kawai Y and Mutai M (1980) Intestinal microflora and bile acids. Effect of bile acids on the distribution of microflora and bile acid in the digestive tract of the rat. *Microbiol Immunol* **24:**187-196.

Setchell KD, Rodrigues CM, Clerici C, Solinas A, Morelli A, Gartung C and Boyer J (1997) Bile acid concentrations in human and rat liver tissue and in hepatocyte nuclei. *Gastroenterology* **112:**226-235.

Staudinger JL, Goodwin B, Jones SA, Hawkins-Brown D, MacKenzie KI, LaTour A, Liu Y, Klaassen CD, Brown KK, Reinhard J, Willson TM, Koller BH and Kliewer SA (2001) The nuclear receptor PXR is a lithocholic acid sensor that protects against liver toxicity. *Proc Natl Acad Sci USA* **98:**3369-3374.

Stedman C, Robertson G, Coulter S and Liddle C (2004) Feed-forward regulation of bile acid detoxification by CYP3A4: studies in humanized transgenic mice. *J Biol Chem* **279:**11336-11343.

Thomas PE, Reik LM, Ryan DE and Levin W (1983) Induction of two immunochemically related rat liver cytochrome P-450 isozymes, cytochromes P-450c and P-450d, by structurally diverse xenobiotics. *J Biol Chem* **258:**4590-4598.

Thomas PJ, Hsia SL, Matschiner JT, Doisy EA, Jr., Elliott WH, Thayer SA and Doisy EA (1964) Bile Acids. Xix. Metabolism of Lithocholic Acid-24-14c in the Rat. *J Biol Chem* **239:**102-105.

Tien ES and Negishi M (2006) Nuclear receptors CAR and PXR in the regulation of hepatic metabolism. *Xenobiotica* **36:**1152-1163.

Voigt W, Thomas PJ and Hsia SL (1968) Enzymic studies of bile acid metabolism. I. 6-beta-Hydroxylation of chenodeoxycholic and taurochenodeoxycholic acids by microsomal preparations of rat liver. *J Biol Chem* **243:**3493-3499.

Wikvall K (1981) Purification and properties of a 3 beta-hydroxy-delta 5-C27-steroid oxidoreductase from rabbit liver microsomes. *J Biol Chem* **256:**3376-3380.

Wong A and Bandiera SM (1996) Inductive effect of Telazol® on hepatic expression of
cytochrome P450 2B in rats. *Biochem Pharmacol* **52:**735-742.

Xie W, Radominska-Pandya A, Shi Y, Simon CM, Nelson MC, Ong ES, Waxman DJ and Evans
RM (2001) An essential role for nuclear receptors SXR/PXR in detoxification of
cholestatic bile acids. Proc Natl Acad Sci USA 98:3375-3380.

Zaki FG, Carey JB, Jr., Hoffbauer FW and Nwokolo C (1967) Biliary reaction and
choledocholithiasis induced in the rat by lithocholic acid. *J Lab Clin Med* 69:737-748.

Zimniak P, Holsztynska EJ, Lester R, Waxman DJ and Radominska A (1989) Detoxification of
lithocholic acid. Elucidation of the pathways of oxidative metabolism in rat liver
microsomes. *J Lipid Res* 30:907-918.

FOOTNOTE:

Figure Legends

Fig. 1. General bile acid structure showing positions available for hydroxylation. The bile acid nomenclature listed in the figure uses trivial names and abbreviations which are similar to that used by Hofmann et al. (1992) and chemical names conform to IUPAC nomenclature.

Fig. 2. Representative LC/MS chromatogram showing metabolites of lithocholic acid extracted from a standard reaction mixture after a 30-min incubation of rat hepatic microsomes (0.5 mg) with 50 µM lithocholic acid and 1 mM NADPH. Metabolite identification was performed by co-chromatography and spiking with authentic standards. The internal standard was deuterated cholic-2,2,4,4-d_4 acid. Peaks identified as β-MCA and HDCA were produced at levels close to or below the limit of quantification. Peaks M-1, M-2, M-3 and M-4 are metabolites that did not correspond to any of the authentic standards. Peaks denoted by * indicate peaks that were present in controls and blanks and are not metabolites.

Fig. 3. Enzyme kinetic profiles of hepatic microsomal MDCA, ILCA and 3KCA formation. Metabolite formation (activity) was plotted as a function of substrate concentration following a 30-min incubation with rat liver microsomes (0.5 mg). Data points are the mean ± SEM of at least three separate experiments. Lines represent rates modeled by nonlinear regression analysis of the data. The insets depict Eadie-Hofstee plots. Error bars are not shown on the insets to avoid obscuring the data points, which represent mean values. Substrate inhibition was observed at lithocholic acid concentrations greater than 100 µM for MDCA formation (A). Sigmoidal kinetics suggestive of homotropic autoactivation were observed for ILCA (B) and 3KCA (C)

formation. Saturating lithocholic acid concentrations of 100 µM and 250 µM were determined

for ILCA and 3KCA formation, respectively.

Fig. 4. Effect of anti-CYP2C IgG and anti-CYP3A IgG on hepatic microsomal MDCA, ILCA

and 3KCA formation. Hepatic microsomes from untreated male rats (0.5 mg) were incubated

with various concentrations of rabbit anti-rat CYP2C polyspecific IgG (–O–), anti-CYP3A

polyspecific IgG (–▼–), and control IgG (–●–) for 15 min at room temperature before addition of

lithocholic acid (100 µM). Results are expressed as percent of the activity obtained in the

presence of 0 mg IgG.

Fig. 5. Comparison of MDCA, ILCA and 3KCA formation by a panel of rat recombinant CYP

enzymes. Metabolite formation (activity) was measured following a 30-min incubation of

lithocholic acid (100 µM) with baculovirus-insect cell microsomes containing expressed rat CYP

enzymes (30 pmol). Insect cell microsomes containing expressed CYP enzymes, except for

CYP1A2 and CYP2D1, also contained co-expressed CYP oxidoreductase and cytochrome b_5.

Microsomes containing expressed CYP1A2 and CYP2D1 contained co-expressed CYP

oxidoreductase but not cytochrome b_5. There was no obvious correlation between rates of

metabolite formation and CYP oxidoreductase or cytochrome b_5 levels in the recombinant CYP

preparations. Plots show the mean values ± SEM of triplicate determinations.

Fig. 6. Enzyme kinetic profile of 3KCA formation by rat recombinant CYP3A2. Metabolite

formation (activity) was plotted as a function of substrate concentration following a 30-min

incubation with rat recombinant CYP3A2 (30 pmoles). The inset depicts an Eadie-Hofstee plot. Data points are the average of duplicate determinations.

Fig. 7. Effect of CYP2D6 antiserum on MDCA formation by rat hepatic microsomes and recombinant CYP2D1. Various amounts of rabbit CYP2D6 antiserum (–●–) or rabbit control serum (–▼–) were added to reaction mixtures (1 ml final volume) containing hepatic microsomes from untreated male rats (0.5 mg). Similarly, various amounts of CYP2D6 antiserum (–O–) or rabbit control serum (–△–) were added to reaction mixtures containing rat recombinant CYP2D1 (30 pmol). Reaction mixtures were preincubated with antibody for 15 min at room temperature before addition of lithocholic acid and initiation of the reaction with NADPH. Results are expressed as percent of the activity obtained in the presence of 0 μl of serum.

Fig. 8. Scheme showing a proposed mechanism for the formation of 3KCA and ILCA from lithocholic acid through a geminal diol intermediate.

Fig. 9. Scheme showing CYP-mediated lithocholic acid biotransformation in rat hepatic microsomes. Results of the present study suggest that MDCA and 3KCA formation was mediated by CYP2C and CYP3A enzymes, and 3KCA formation was mediated by CYP2C and CYP3A enzymes, whereas ILCA formation was mediated largely by non-CYP enzymes. The CYP enzymes mediating formation of minor lithocholic acid metabolites (i.e. β-MCA, UDCA and 6KLCA) were not identified.

31

TABLE 1. Kinetic parameters of lithocholic acid metabolite formation by

rat hepatic microsomes

Metabolite	Apparent V_{max} pmol/min/mg protein	Apparent K_m μM	Apparent K' μM	n	Apparent K_i μM
MDCA[a]	5920 ± 1180	56.0 ± 17.8	N/A	N/A	194 ± 74.6
ILCA[b]	803 ± 91.8	N/A	29.3 ± 5.9	2.3 ± 0.8	N/A
3KCA[b]	413 ± 25.8	N/A	71.6 ± 6.5	2.5 ± 0.6	N/A
6KLCA[c]	44.5 ± 2.1	1.6 ± 0.3	N/A	N/A	N/A
UDCA[c]	22.4 ± 1.7	15.3 ± 3.7	N/A	N/A	N/A

Kinetic parameters were derived from the metabolite formation data presented in Fig. 3. Values

represent the mean ± SEM of triplicate determinations.

[a] Kinetic parameters for MDCA formation were calculated using the substrate inhibition kinetics

model (equation 2).

[b] Kinetic parameters for ILCA and 3KCA formation were calculated using the sigmoidal

kinetics model, Hill equation (equation 1).

[c] Kinetic parameters for 6KLCA and UDCA formation were calculated using the Michaelis-

Menten equation.

N/A, not applicable

TABLE 2. Effect of sex and treatment with CYP inducers on lithocholic acid metabolite

formation by rat hepatic microsomes

Treatment	Rate of metabolite formation *pmol/min/mg protein*		
	MDCA	ILCA	3KCA
Male rats			
Control	2900 ± 302	803 ± 83.0	512 ± 49.7
MC	$1010 \pm 171^*$	$403 \pm 70.0^*$	486 ± 117
PB	$633 \pm 150^*$	$231 \pm 55.0^*$	394 ± 106
DEX[a]	1810	765	1380
Female rats			
Control	$1220 \pm 182^*$	$25.3 \pm 1.4^*$	461 ± 19.0
PB[a]	1250	23.2	585
DEX	781 ± 122	33.2 ± 10.0	1050 ± 169

Incubation of hepatic microsomes with lithocholic acid was carried out at saturating

substrate concentrations (100 μM lithocholic acid for MDCA and ILCA and 250 μM for

3KCA, respectively) under optimal assay conditions as described in the Materials and

Methods section. Hepatic microsomes prepared from vehicle-treated male and untreated

female Long-Evans rats were used as controls. Values represent the mean ± SEM of

triplicate determinations, except for treatments denoted by [a], where values represent the

average of duplicate determinations. Rates of metabolite formation for hepatic microsomes prepared from male rats pretreated with MC or PB and from control female rats were compared to rates obtained with hepatic microsomes prepared from control male rats (*, $p < 0.05$). Rates of metabolite formation for hepatic microsomes prepared from female rats pretreated with DEX were compared to rates obtained with hepatic microsomes prepared from control female rats ($p < 0.07$).
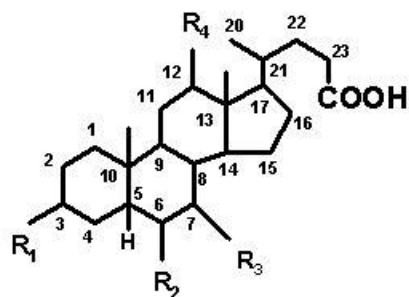
|	R$_1$	R$_2$	R$_3$	R$_4$	Bile acid/metabolite	Chemical name
1.	α-OH	H	H	H	lithocholic acid	5β-cholanic acid-3α-ol
2.	α-OH	H	α-OH	H	chenodeoxycholic acid (CDCA)	5β-cholanic acid-3α, 7α-diol
3.	α-OH	H	α-OH	α-OH	cholic acid	5β-cholanic acid-3α, 7α, 12α-triol
4.	α-OH	β-OH	α-OH	H	α-muricholic acid (α-MCA)	5β-cholanic acid-3α, 6β, 7α-triol
5.	α-OH	β-OH	β-OH	H	β-muricholic acid (β-MCA)	5β-cholanic acid-3α, 6β, 7β-triol
6.	α-OH	α-OH	H	H	hyodeoxycholic acid (HDCA)	5β-cholanic acid-3α, 6α-diol
7.	α-OH	β-OH	H	H	murideoxycholic acid (MDCA)	5β-cholanic acid-3α, 6β-diol
8.	O	H	H	H	3-ketocholanoic acid (3KCA)	5β-cholanic acid-3-one
9.	α-OH	O	H	H	6-ketolithocholic acid (6KLCA)	5β-cholanic acid-3α-ol-6-one
10.	β-OH	H	H	H	isolithocholic acid (ILCA)	5β-cholanic acid-3β-ol
11.	α-OH	H	β-OH	H	ursodeoxycholic acid (UDCA)	5β-cholanic acid-3α, 7β-diol
12.	α-OH	H	H	α-OH	deoxycholic acid	5β -cholanic acid-3β, 12α -diol

Figure 1
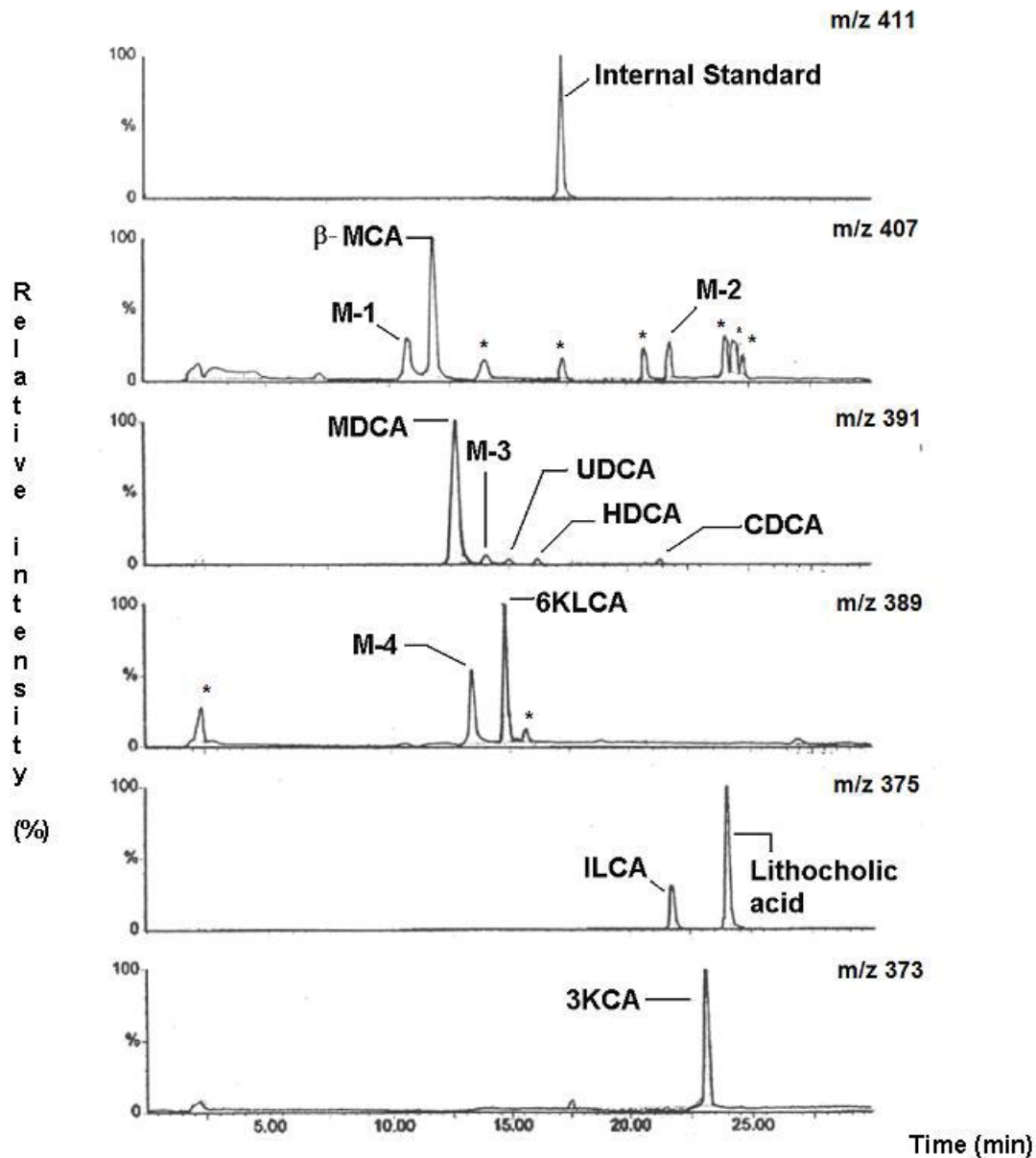
Figure 2
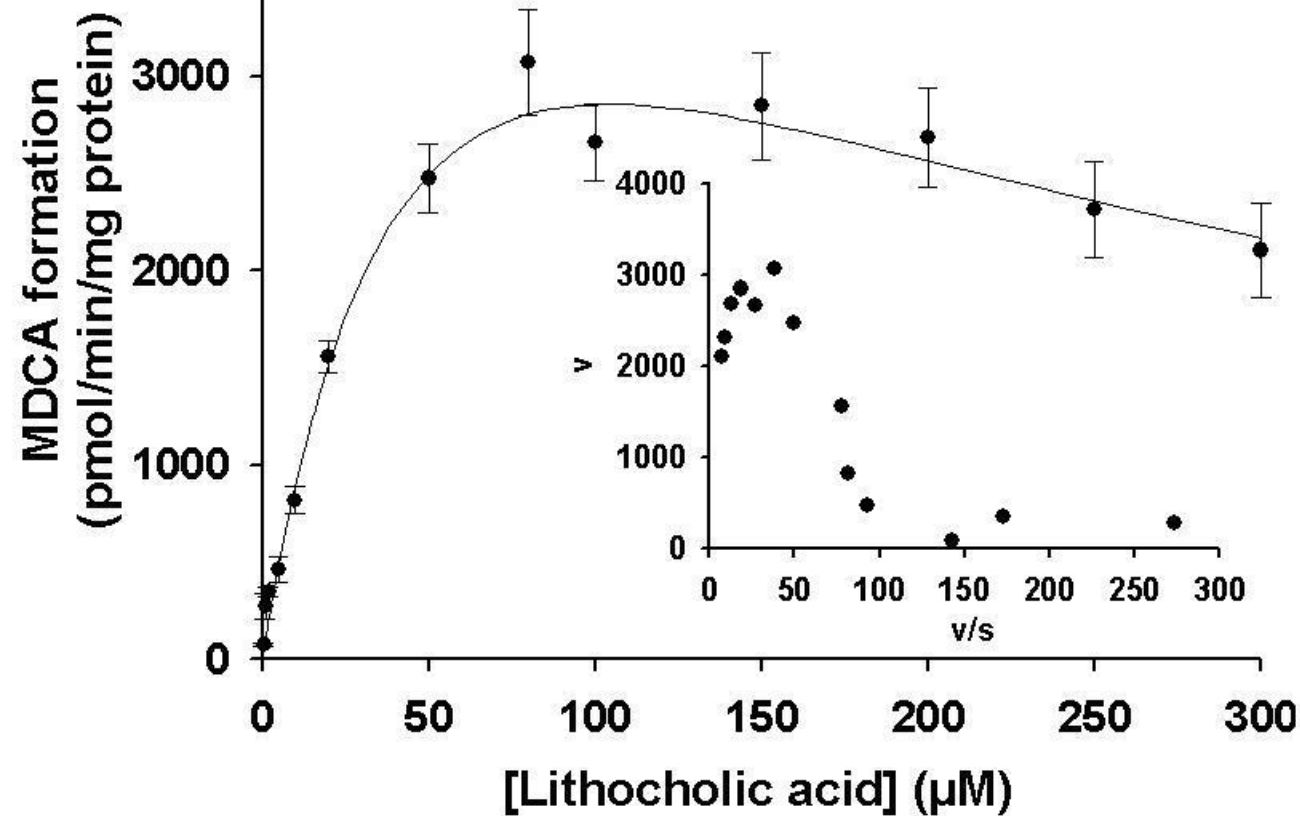
Figure 3A
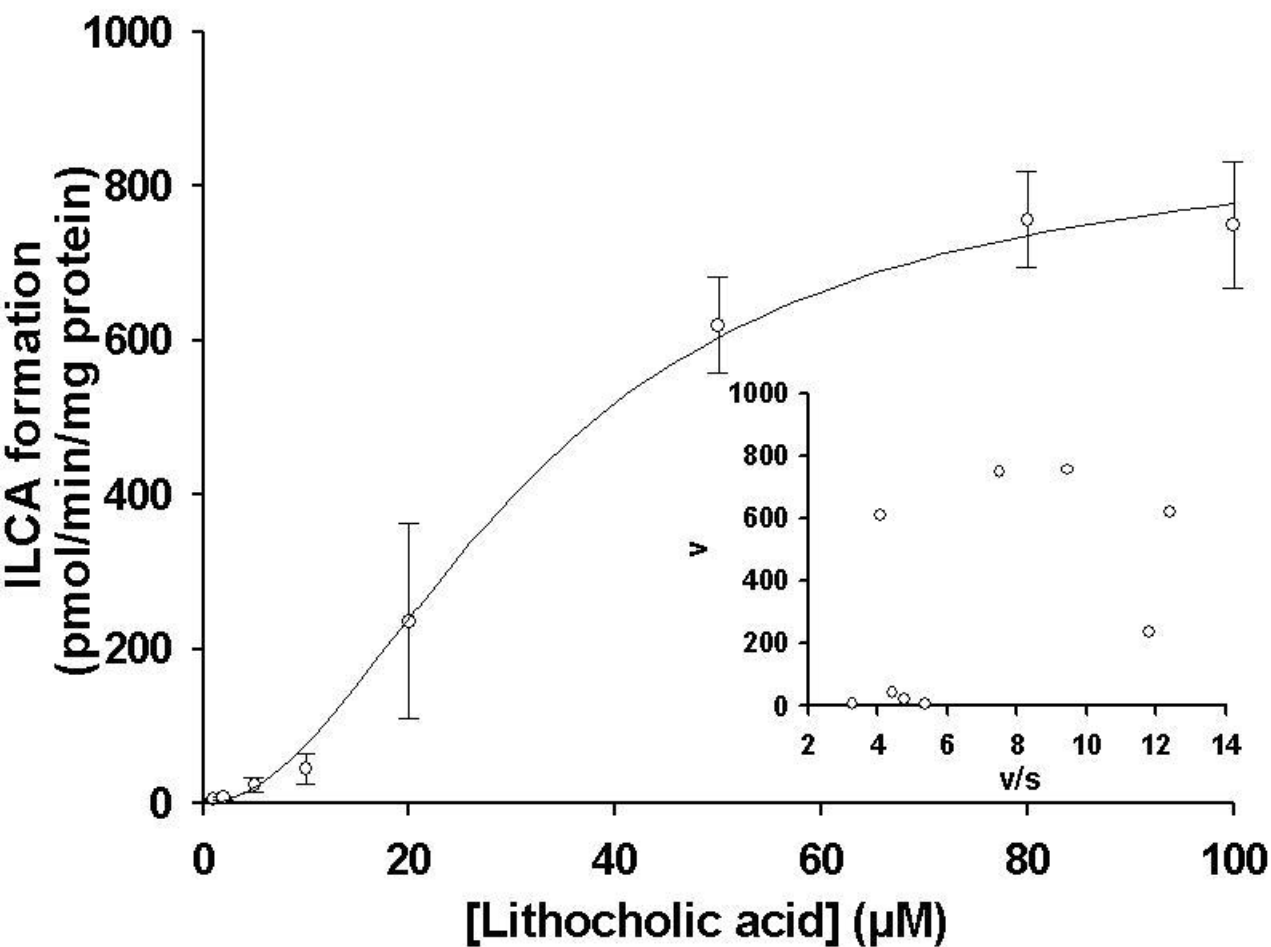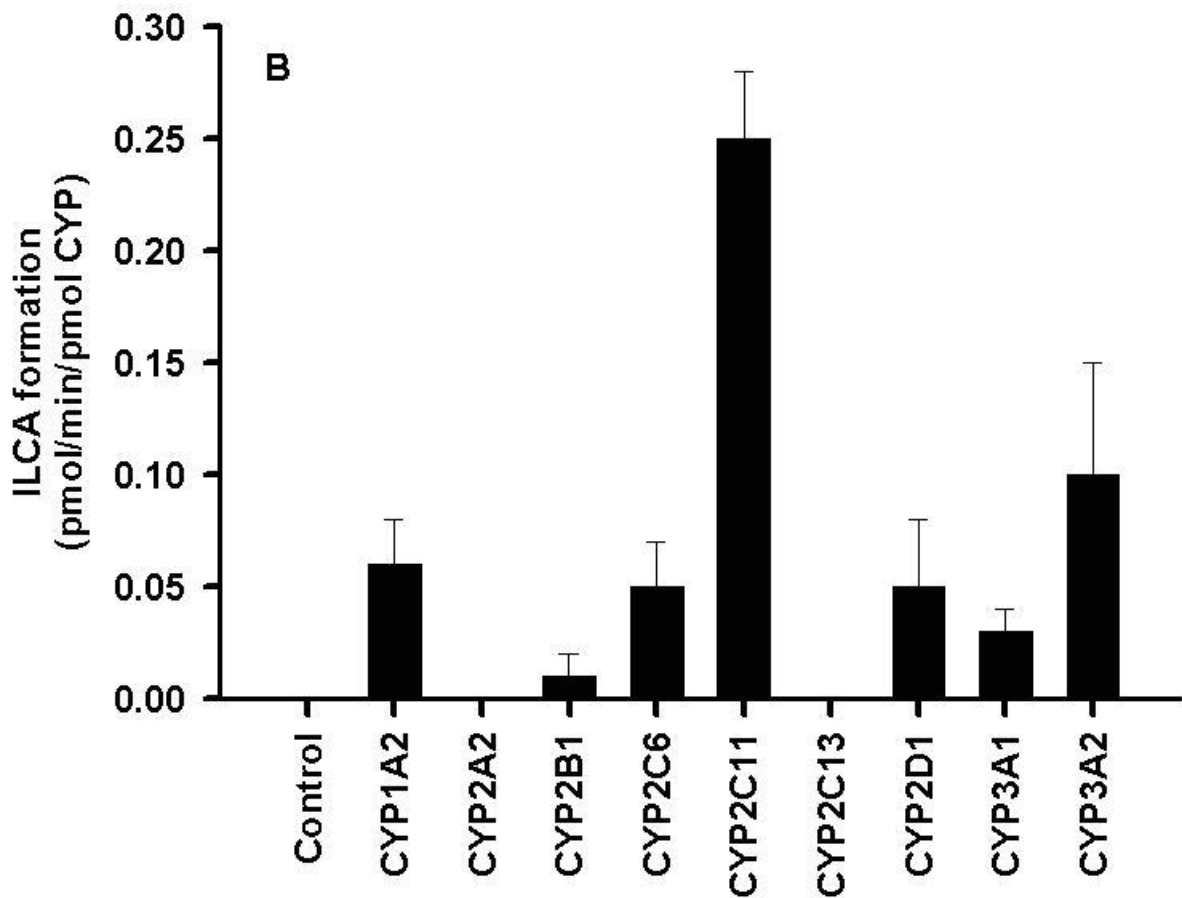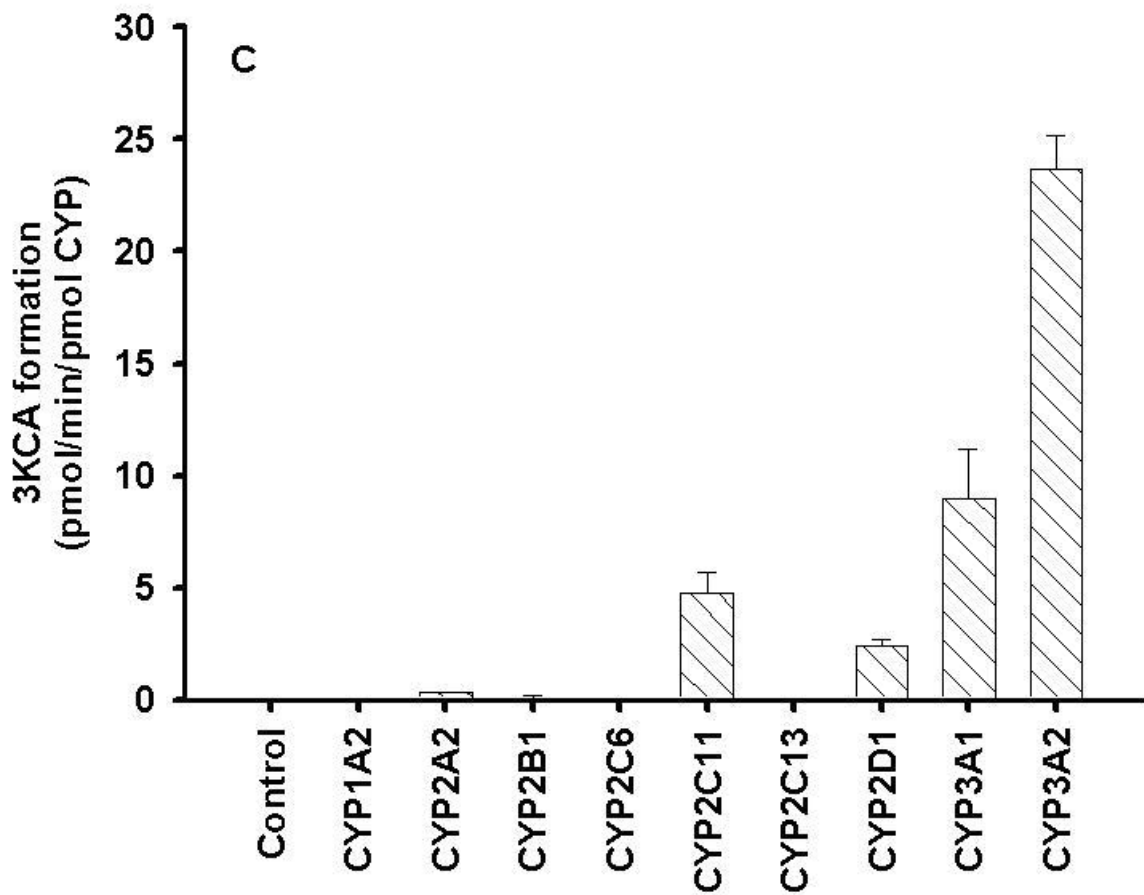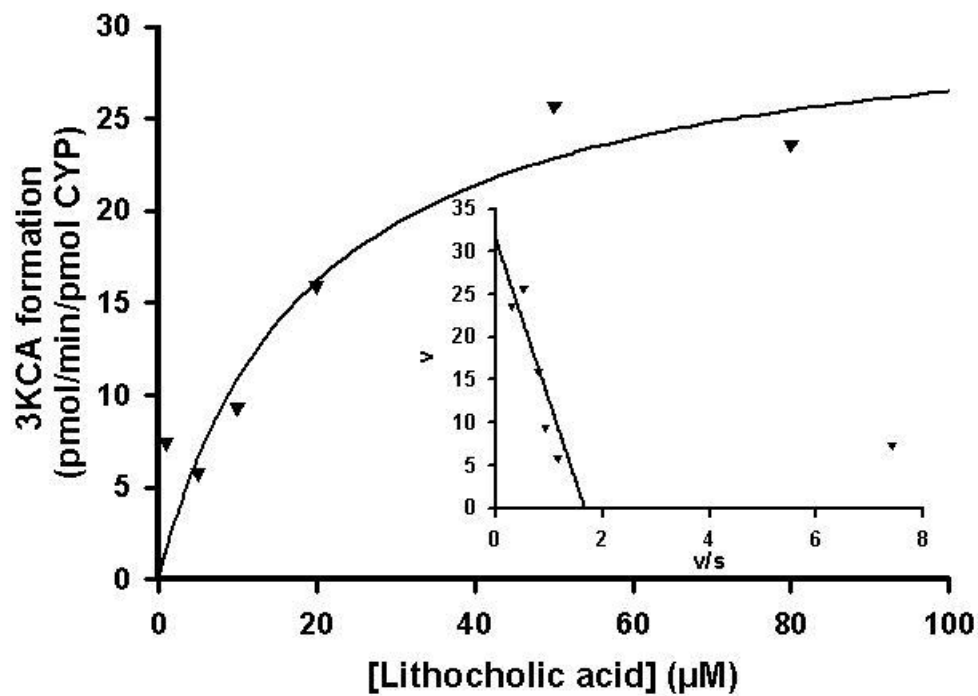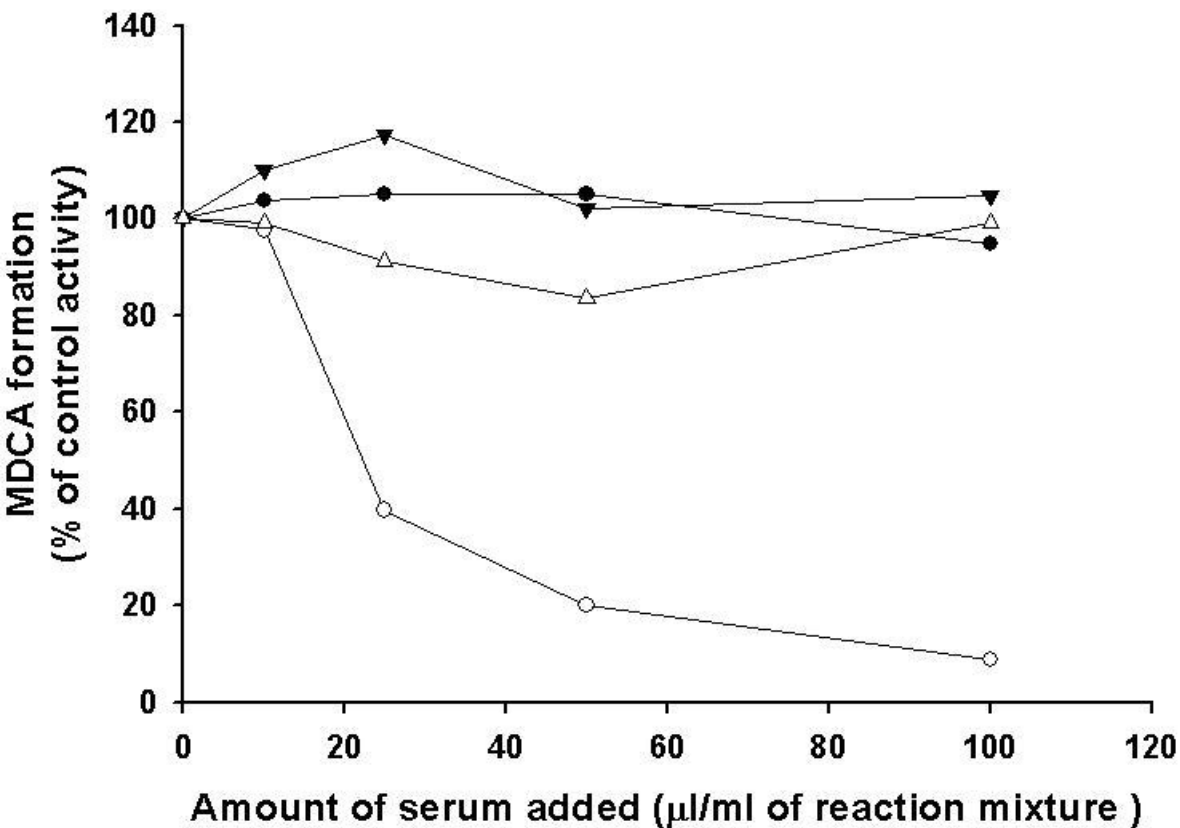
Figure 3B
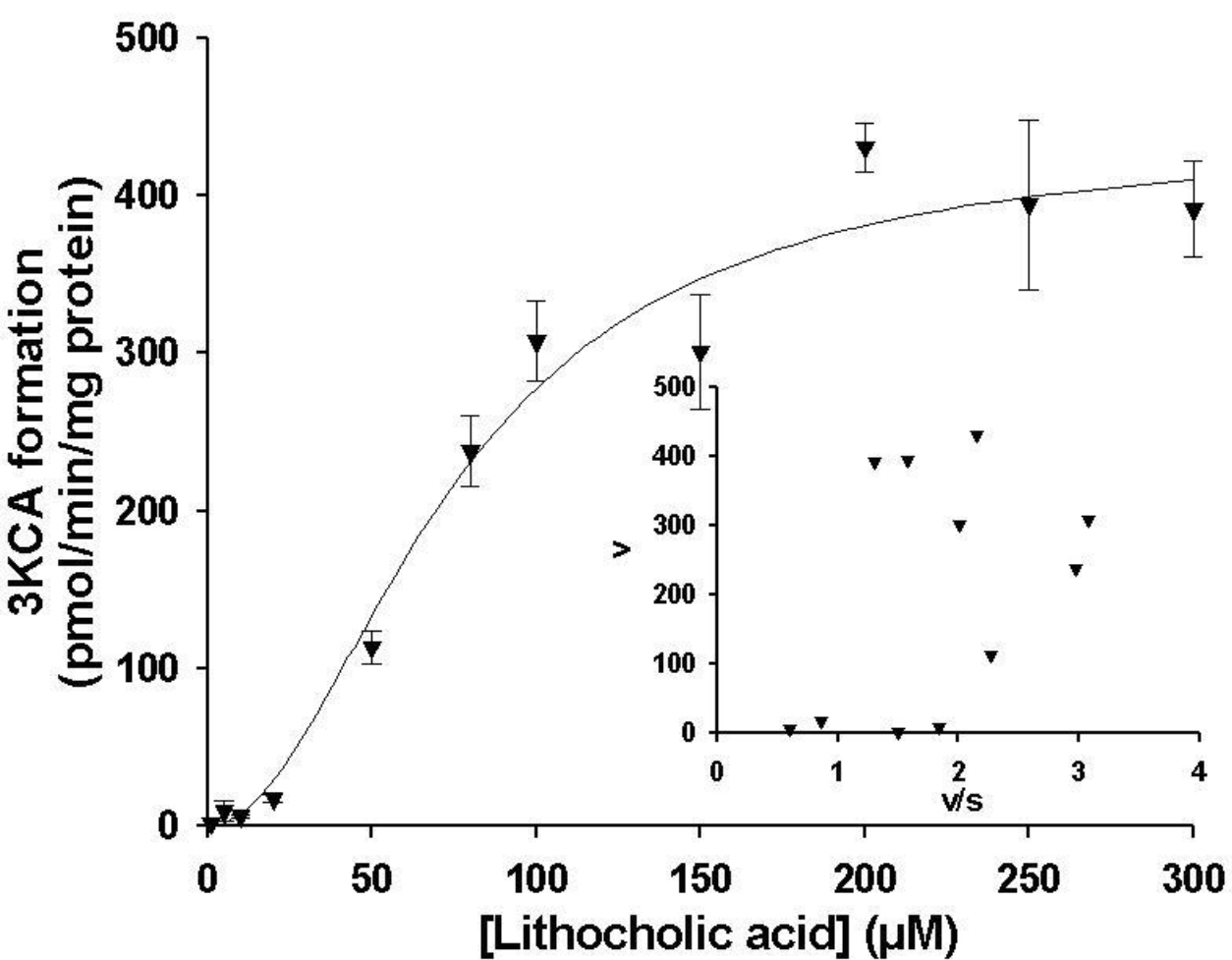
Figure 3C
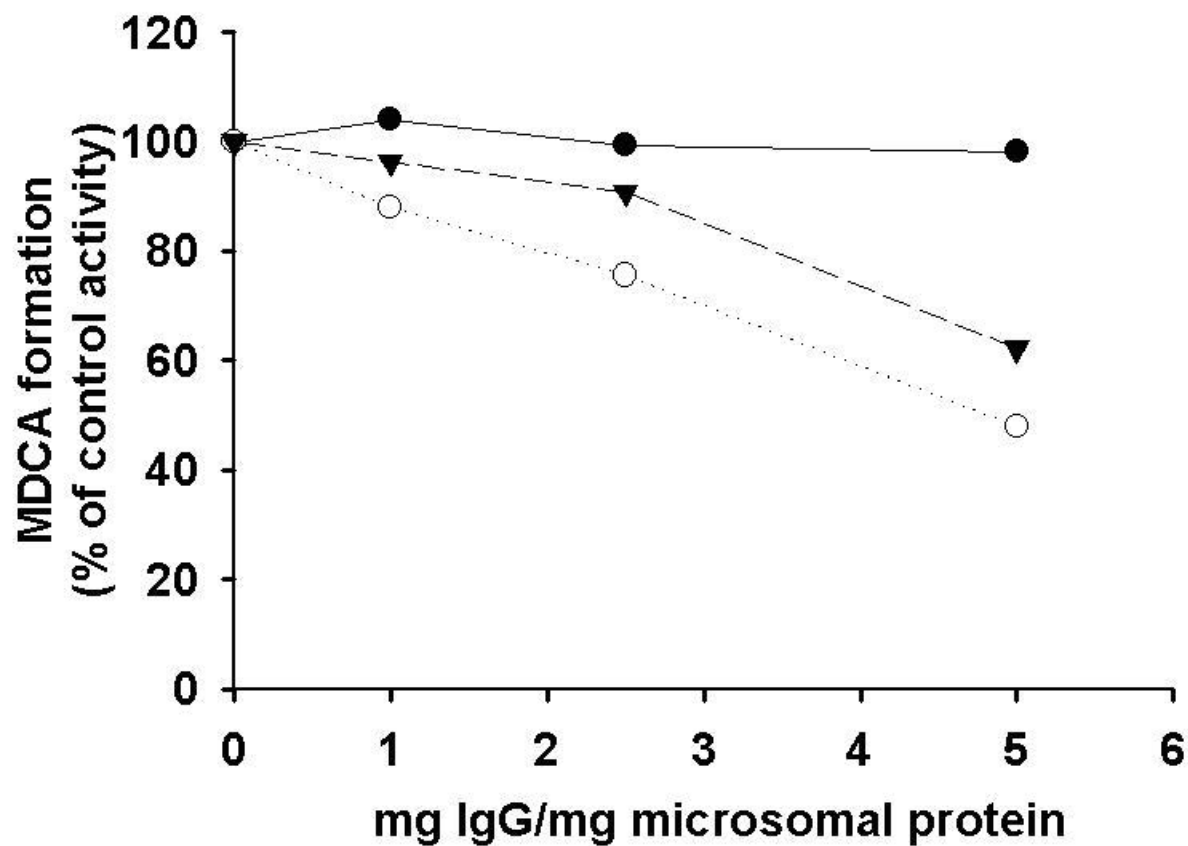
Figure 4A
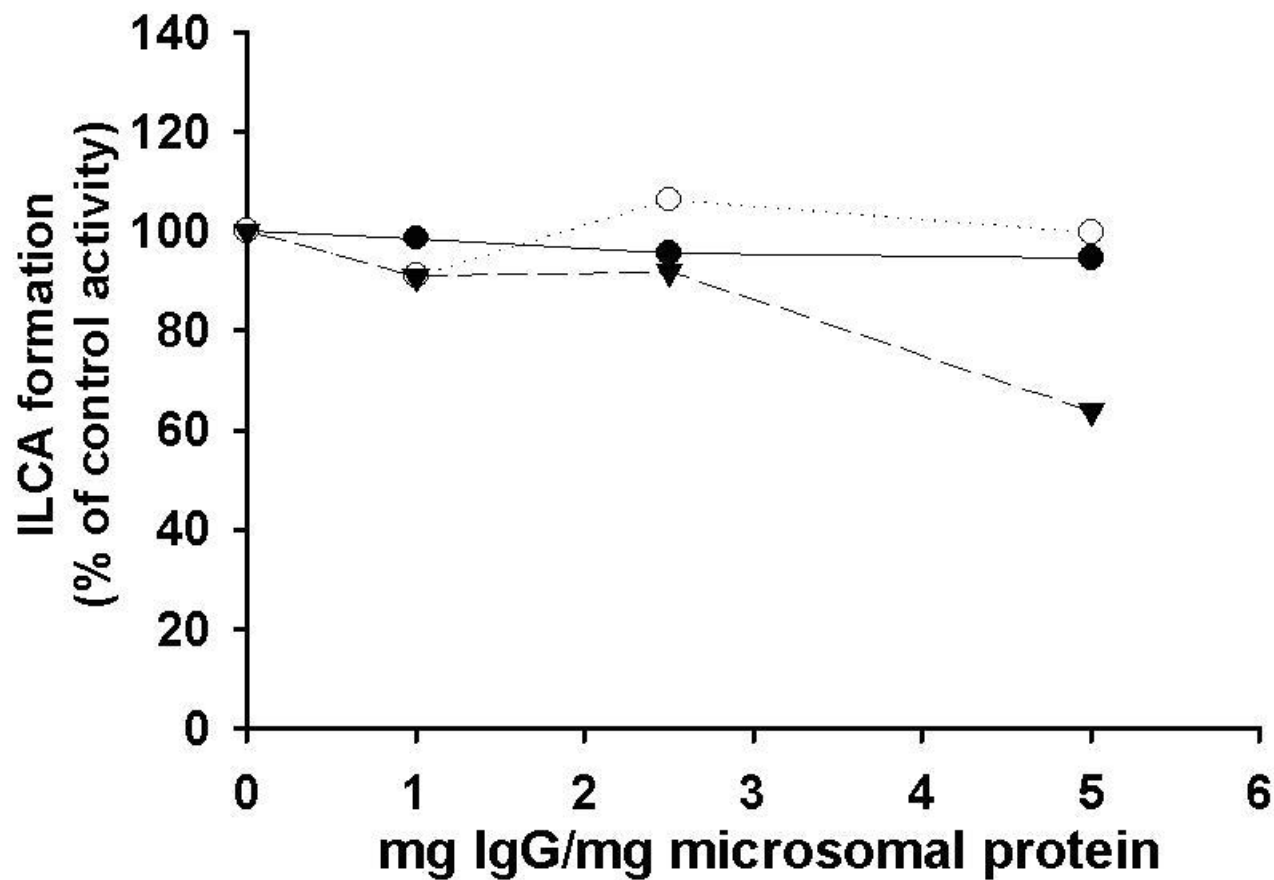
Figure 4B
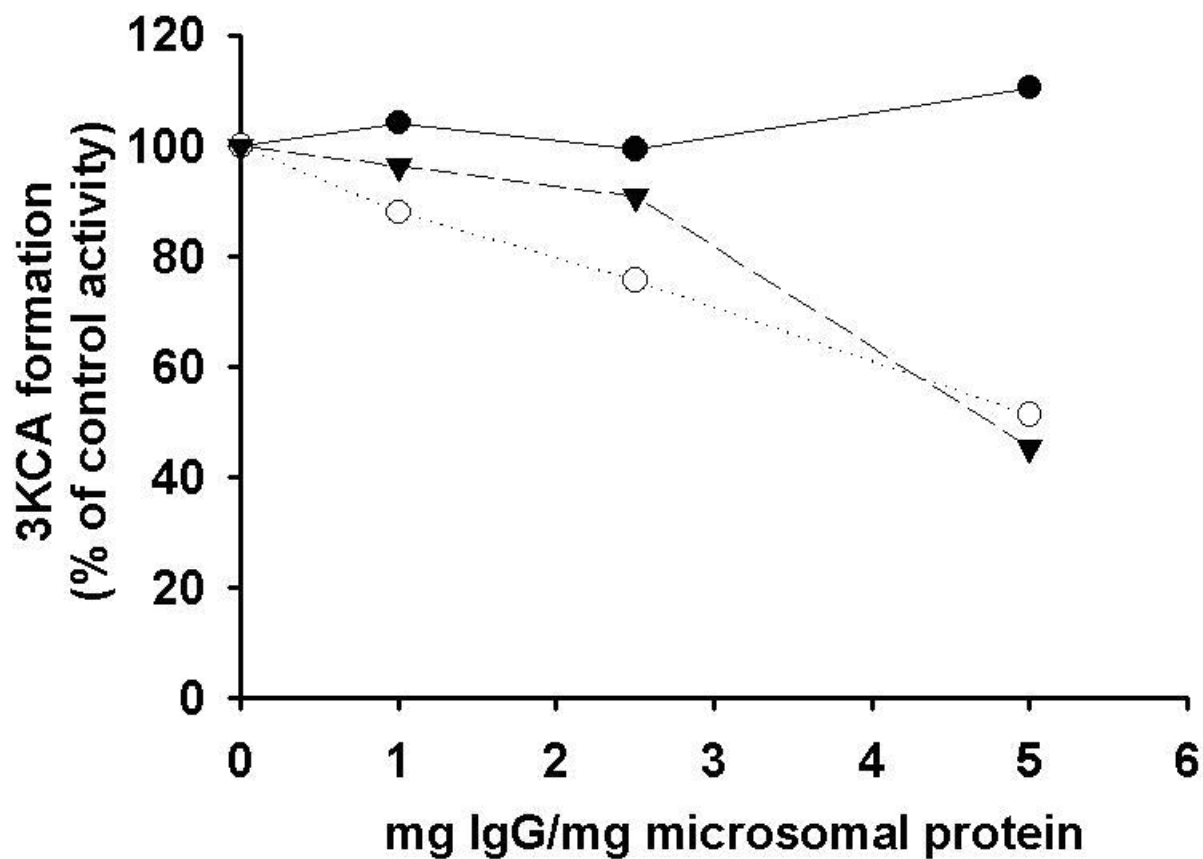
Figure 4C
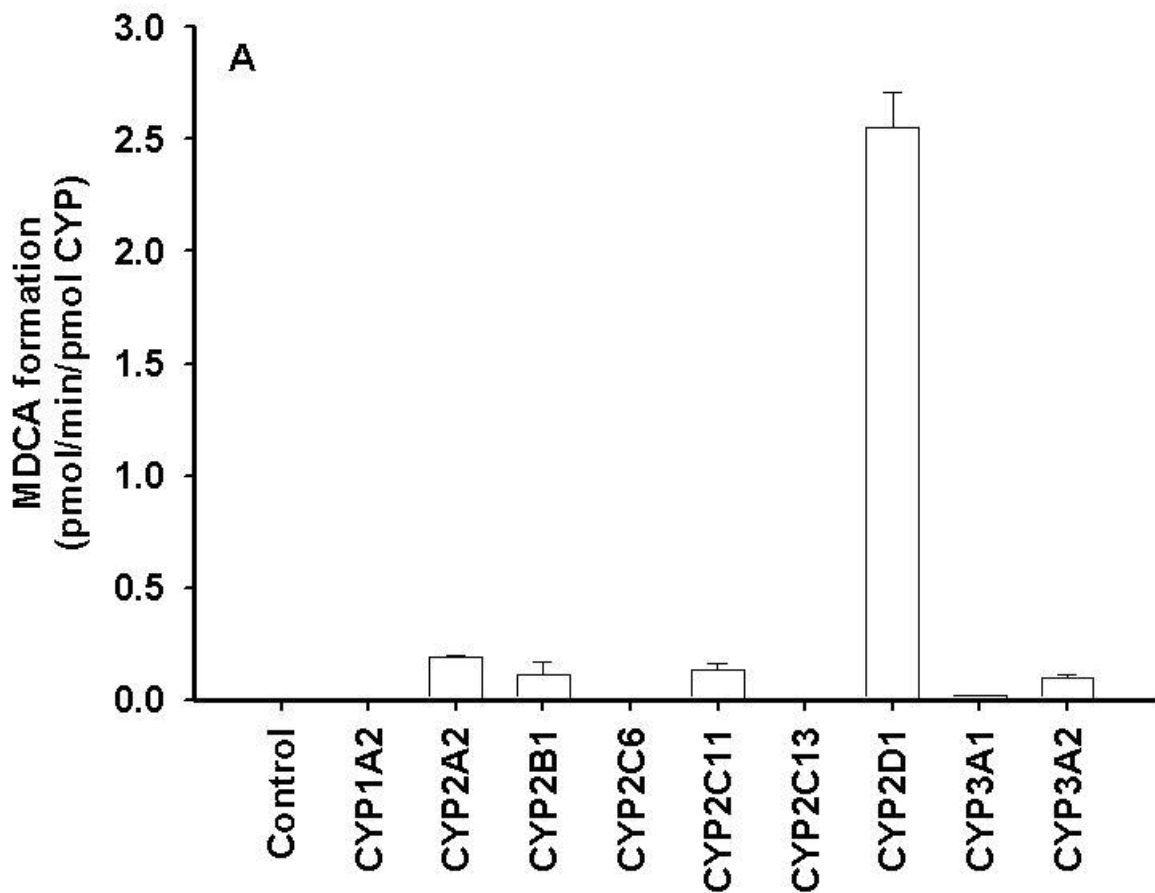
Figure 5A

Figure 5B

Figure 5C

Figure 6

Figure 7

Figure 8

Figure 9